

Exploring Fluorescence Antibunching in Solution To Determine the Stoichiometry of Molecular Complexes

Jan Sýkora,^{†,‡} Karin Kaiser,[§] Ingo Gregor,[†] Wolfgang Bönigk,[†] Günther Schmalzing,[§] and Jörg Enderlein^{*,†,||}

Institute for Neuroscience and Biophysics 1, Forschungszentrum Jülich, D 52425 Jülich, Germany, J. Heyrovský Institute of Physical Chemistry, Academy of Sciences of the Czech Republic, Dolejškova 3, 18223 Praha 8, Czech Republic, Aachen University, D-52074 Aachen, Germany, and Institute of Physical and Theoretical Chemistry, Eberhard Karls University Tübingen, D-72076 Tübingen, Germany

Fluorescence antibunching is a well-known technique for determining the number of independent emitters per molecule or molecular complex. It was rarely applied to autofluorescent proteins due to the necessity of collecting large numbers of fluorescence photons from a single molecule, which is usually impossible to achieve with rather photolabile autofluorescent proteins. Here, we measure fluorescence antibunching on molecules in solution, allowing us to accumulate data over a large number of molecules. We use that method for determining an average stoichiometry of molecular complexes. The proposed method is absolute in the sense that it does not need any calibration or referencing. We develop the necessary theoretical background and check the method on pure dye solutions and on molecular complexes with known stoichiometry.

Determination of the stoichiometry of molecular complexes is an important issue in biological studies. Many functional units in cells such as ion channels, molecular motors, and enzymatic complexes are composed of several protein subunits. Knowing the exact stoichiometry of these complexes, i.e., the numbers of identical or similar molecular units that form a complex, is important for understanding their structure and functioning.

A classical biophysical method for the characterization of interactions of purified proteins in dilute solutions is analytical ultracentrifugation; see, for example, refs 1 and 2^{1,2}. However, this method requires protein in the order of a few hundred micrograms of greater than 95% purity, which makes the method very time-consuming and labor intensive, particularly with membrane proteins. In recent years, new single-molecule fluorescence-based methods have been developed that are potentially able to determine stoichiometry of molecular complexes by measuring

the fluorescence brightness on the level of a single complex. This idea was pioneered by Keller and his group: using a modified single-molecule sensitive flow cytometer,^{3,4} they were able to classify single molecules by determining the number of fluorescence photons emitted during directed and controlled transport through a laser focus.⁵ They successfully applied the technique for, for example, rapid DNA fragment sizing.^{6–8} The main advantage of the flow cytometer system was that every molecule took a nearly identical path through the detection region. Thus, the number of detected fluorescence photons per molecule was nearly the same for all molecules of one species. Although the flow cytometer delivers excellent data, the setup has been too complicated and fragile to find widespread application. Nowadays, single-molecule detection is usually done using a confocal epifluorescence microscope.⁹ Here, the molecules are diffusing freely and therefore their transits through the detection region are stochastic in nature. Consequently, each single-molecule transit will deliver a different number of fluorescence photons. However, by applying a statistical analysis to the distribution of numbers of detected photons per time unit, one can find values for the average fluorescence brightness or even for distributions of brightness values when more than a single species of fluorescent molecules is present. This method was independently developed by two groups and called photon count histogramming (PCH)^{10,11} or

* To whom correspondence should be addressed. Fax: (+) (49)-7071-29-76911. E-mail: joerg.enderlein@uni-tuebingen.de. Internet: www.joerg-enderlein.de.

[†] Institute for Neuroscience and Biophysics 1.

[‡] J. Heyrovský Institute of Physical Chemistry.

[§] Aachen University.

^{||} Eberhard Karls University Tübingen.

(1) Schubert, D.; Schuck, P. *Prog. Colloid Polym. Sci.* **1991**, *86*, 12–22.

(2) Schuck, P.; Perugini, M. A.; Gonzales, N. R.; Howlett, G. J.; Schubert, D. *Biophys. J.* **2002**, *82*, 1096–1111.

(3) Dovichi, N. J.; Martin, J. C.; Jett, J. H.; Keller, R. A. *Science* **1983**, *219*, 845–847.

(4) Goodwin, P. M.; Ambrose, W. P.; Keller, R. A. *Acc. Chem. Res.* **1996**, *29*, 607–613.

(5) Machara, N. P.; Goodwin, P. M.; Semin, D.; Enderlein, J.; Keller, R. A. *Bioimaging* **1998**, *6*, 33–42.

(6) Goodwin, P. M.; Johnson, M. E.; Martin, J. C.; Ambrose, W. P.; Marrone, B. L.; Jett, J. H.; Keller, R. A. *Nucleic Acids Res.* **1993**, *21*, 803–806.

(7) Goodwin, P. M.; Cai, H.; Jett, J. H.; Ishaug-Riley, S. L.; Machara, N. P.; Semin, D. J. A. Van Orden; Keller, R. A. *Nucleosides Nucleotides* **1997**, *16*, 534.

(8) Davis, L. M.; Fairfield, F. R.; Harger, C. A.; Jett, J. H.; Keller, R. A.; Hahn, J. H.; Krakowski, L. A.; Marrone, B. L.; Martin, J. C.; Nutter, H. L.; Ratliff, R. L.; Shera, E. B.; Simpson, D. J.; Soper, S. A. *GATA* **1991**, *8*, 1–7.

(9) Böhmer, M.; Enderlein, J. Single molecule detection on surfaces with the confocal laser scanning microscope. In *Single-Molecule Detection in Solution: Methods and Applications*; Zander, C., Enderlein, J., Keller, R. A., Eds.; VCH-Wiley: Berlin, 2002; pp 145–183.

(10) Chen, Y.; J. D. Müller, P. T.; So, C.; Gratton, E. *Biophys. J.* **1999**, *77*, 553–567.

(11) Müller, J. D.; Chen, Y.; Gratton, E. *Biophys. J.* **2000**, *78*, 474–486.

fluorescence intensity distribution analysis (FIDA),^{12,13} respectively. Although these methods have been successfully applied for estimating fluorescence brightness values of individual molecules^{14,15} or studying protein association,¹⁶ their application can be challenging: First, for counting single emitters in a complex based on brightness using PCH or FIDA, one needs to calibrate against a solution of pure monomers of the used fluorescent label. Second, signal strength, high background, and the presence of photobleaching require improved statistical analysis.¹⁷

With the advent of single-molecule imaging,^{18–20} it became possible to directly measure the fluorescence brightness of single immobilized molecules and, thus, to count number of molecules on one spot.²¹ The major problem with this approach is that the presence of a binding surface or an embedding polymer usually strongly affects the photophysical properties of a fluorescing molecule, so that practically each molecule shows a different fluorescence brightness.

A powerful and gauge-free technique for obtaining information on the number of independently fluorescing dye molecules within a complex is fluorescence antibunching.²² Photon antibunching is the effect that a single photon emitter such as a fluorescent molecule cannot emit more than a single photon at any given time. Therefore, the occurrence of photon pairs from a single molecule detected within a given lag time between them tends to zero with the lag time approaching zero. The characteristic lag time of this drop is determined by the fluorescence lifetime of the molecule. If more than a single molecule is present, the drop will not go to zero but to a larger value that is determined by the exact number of independently fluorescing molecules within the detection volume. Thus, antibunching allows for the determination of the number of independently emitting molecules within a molecular complex, and it was successfully applied for that purpose in measurements on immobilized molecules.^{23–27} The drawback of this method is the need of high count rates and photostable

molecules to obtain sufficiently good antibunching data, which makes this method rather difficult to apply for autofluorescent proteins, which are widely used for protein labeling.

A way of circumventing photobleaching and low signal strength in antibunching measurements is to measure in solution and to accumulate signal over many molecule transits through the detection volume. Although antibunching measurements on fluorescent molecules diffusing in solution were successfully demonstrated as early as 1985,²⁸ to our knowledge, it was never applied for determining the number of independently fluorescing molecules on a diffusing complex. Here, we briefly recall the necessary theoretical background and present antibunching measurement on pure dye solutions and multiply labeled molecular complexes.

THEORY

We briefly recall the theoretical basis of fluorescence autocorrelation measurements, paying special attention to its structure on a time scale comparable with the fluorescence lifetime of a molecule. The fluorescence autocorrelation probes the probability to detect a photon after some time t (lag time) if there was a photon detection event at time zero, and it has the general form

$$g(t) = cg_1(t) + [c\bar{f} + b]^2 \quad (1)$$

where c is the concentration of molecules in the solution, $g_1(t)$ is the one-molecule fluorescence correlation function for photons emitted by one and the same molecule, and \bar{f} and b are the average fluorescence signal of a single molecule and the background intensity (scattered light, detector and electronic noise), respectively. Please note that the autocorrelation function $g(t)$ as presented in eq 1 is un-normalized: In many publications, and also in all autocorrelation figures of this paper, $g(t)$ is shown normalized by its value at $t = \infty$. The one-molecule correlation function g_1 can be written as the product of detecting a photon at time zero times the conditional probability to detect a next photon from the same molecule at time t . Let us start with considering g_1 on short time scales, during which the position of the molecule within the laser focus does not change sensibly, so that g_1 is only determined by the photophysical processes of the labels. Assume that every diffusing molecule is tagged with n independent fluorescing labels (dipole emitters). The probability to detect, from such a molecule, a photon at any time is given by the average stationary fluorescence detection rate $n\langle f_s(\mathbf{r}) \rangle_r$, where $f_s(\mathbf{r})$ is the average stationary detection rate for single label at position \mathbf{r} , and the angular brackets with subscript \mathbf{r} denote averaging over all possible positions \mathbf{r} of a molecule in space. The function $f_s(\mathbf{r})$ depends on local excitation light intensity and polarization, the

- (12) Kask, P.; Palo, K.; Ullmann, D.; Gall, K. *Proc. Nat. Acad. Sci. U.S.A.* **1999**, *96*, 13756–13761.
- (13) Palo, K.; Mets, U.; Jäger, S.; Kask, P.; Gall, K. *Biophys. J.* **2000**, *79*, 2858–2866.
- (14) Chen, Y. J.; Müller, D.; QiaoQiao, R.; Gratton, E. *Biophys. J.* **2002**, *82*, 133–144.
- (15) Haupts, U. M.; Rüdiger, S.; Ashman, S.; Turconi, R.; Bingham, C.; Wharton, J.; Hutchinson, C.; Carey, K.; Moore, J.; Pope, A. J. *J. Biomol. Screening* **2003**, *8*, 19–33.
- (16) Chen, Y.; Wei, L. N.; Müller, J. D. *Proc. Nat. Acad. Sci. U.S.A.* **2003**, *26*, 15492–15497.
- (17) Wu, B.; Müller, J. D. *Biophys. J.* **2005**, *89*, 2721–2735.
- (18) Sase, I.; Miyata, H.; Corrie, J. E.; Craik, J. S.; Kinoshita, K. *Biophys. J.* **1995**, *69*, 323–328.
- (19) Funatsu, T.; Harada, Y.; Tokunaga, M.; Saito, K.; Yanagida, T. *Nature* **1995**, *374*, 555–559.
- (20) Schmidt, T. G.; Schütz, J.; Baumgärtner, W.; Gruber, H. J.; Schindler, H. *Proc. Nat. Acad. Sci. U.S.A.* **1996**, *93*, 2926–2929.
- (21) Schmidt, T. G.; Schütz, J.; Gruber, H. J.; Schindler, H. *Anal. Chem.* **1996**, *68*, 4397–4401.
- (22) Ambrose, W. P.; Goodwin, P. M.; Enderlein, J.; Semin, D. J.; Martin, J. C.; Keller, R. A. *Chem. Phys. Lett.* **1997**, *269*, 365–370.
- (23) Tinnefeld, P.; Weston, K. D.; Vosch, T.; Cotlet, M.; Weil, T.; Hofkens, J.; Müllen, K.; De Schryver, F. C.; Sauer, M. *J. Am. Chem. Soc.* **2002**, *124*, 14310–14311.
- (24) Weston, K. D.; Dyck, M.; Tinnefeld, P. C. Müller, D.; Herten, P.; Sauer, M. *Anal. Chem.* **2002**, *74*, 5342–5349.
- (25) Tinnefeld, P.; Buschmann, V.; Weston, K. D.; Sauer, M. *J. Phys. Chem. A* **2003**, *107*, 323–327.
- (26) Tinnefeld, P.; Hofkens, J.; Herten, D. P.; Masuo, S.; Vosch, T.; Cotlet, M.; Habuchi, S.; Müllen, K.; De Schryver, F. C.; Sauer, M. *ChemPhysChem* **2004**, *5*, 1796–1790.

- (27) Masuo, S.; Vosch, T.; Cotlet, M.; Tinnefeld, P.; Habuchi, S.; Bell, T. D. M.; Oesterling, I.; Beljonne, D.; Champagne, B.; Müllen, K.; Sauer, M.; Hofkens, J.; De Schryver, F. C. *J. Phys. Chem. B* **2004**, *108*, 16686–16696.
- (28) Kask, P.; Piksarv, P.; Mets, Ü. *Eur. Biophys. J.* **1985**, *12*, 163–166.
- (29) Hofkens, J.; Cotlet, M.; Vosch, T.; Tinnefeld, P.; Weston, K. D.; Ego, C.; Grimsdale, A. K.; Müllen, D.; Beljonne, J.; Brédas, L.; Jordens, S.; Schweitzer, G.; Sauer, M.; De Schryver, F. C. *Proc. Nat. Acad. Sci. U.S.A.* **2003**, *100*, 13146–13151.
- (30) Vosch, T.; Cotlet, M.; Hofkens, J.; Der Biest Van, K.; Lor, M.; Weston, K.; Tinnefeld, P.; Sauer, M.; Latterini, L.; Müllen, K.; De Schryver, F. C. *J. Phys. Chem. A* **2003**, *107*, 6920–6931.

labels' photophysics, and the optical light detection in a complex manner. Stationary $f_s(\mathbf{r})$ means that all photophysically relevant states of a label (ground state, first singlet excited state, triplet state, etc.) are in stationary equilibrium with the exciting light intensity. In contrast, after the emission of a photon (say at time $t = 0$), the label starts in the ground state and its fluorescence emission rate is a function of time, generally described by

$$f(\mathbf{r}, t) = f_s(\mathbf{r}) + \sum_j c_j(\mathbf{r}) \exp(-\lambda_j t) \quad (2)$$

where the λ_j are the (positive) characteristic roots of the photophysical rate equations and the c_j are constants determined by the local excitation light intensity (and polarization) at position \mathbf{r} . Furthermore, without having to know the explicit form of the λ_j and c_j , $f(\mathbf{r}, t)$ has to be zero at zero time, because a fluorophore needs time to be excited from the ground into the excited state before it can emit a photon. For almost all fluorescent dyes used in FCS experiments, the relaxation of $f(\mathbf{r}, t)$ toward its stationary value $f_s(\mathbf{r})$ happens on a time scale between nanoseconds and a few microseconds, where diffusion of the molecules within the spatially nonuniform distribution of excitation light intensity is negligible. On this short time scale, the g_1 reads

$$g_1(t) = \langle n f(\mathbf{r}, t) f_s(\mathbf{r}) + n(n-1) f_s^2(\mathbf{r}) \rangle_r \quad (3)$$

where it has been taken into account that there are n possibilities that a photon pair is emitted by the same of the n labels and $n(n-1)$ possibilities that it is emitted by different labels. On longer time scales, after relaxation of the photophysics to stationary conditions and diffusion sets in, g_1 takes the standard form

$$g_1(t) = n^2 \langle f_s(\mathbf{r}_1) G(\mathbf{r}_1 - \mathbf{r}_0, t) f_s(\mathbf{r}_0) \rangle_{\mathbf{r}_0, \mathbf{r}_1} \quad (4)$$

where $G(\mathbf{r}_1 - \mathbf{r}_0, t)$ is the probability density that a molecule diffuses from position \mathbf{r}_0 to position \mathbf{r}_1 within time t (Green's function of the diffusion equation), which decays to zero for large values of t . For obtaining information about the number n of labels on the diffusing molecules, three values of the autocorrelation function (ACF) are important: Its limiting value when lag time t tends to zero,

$$g_0 \equiv \lim_{t \rightarrow 0} g(t) = cn(n-1) \langle f_s^2(\mathbf{r}) \rangle_r + (b + cn \langle f_s(\mathbf{r}) \rangle_r)^2 \quad (5)$$

its limit at infinite lag time,

$$g_\infty \equiv \lim_{t \rightarrow \infty} g(t) = (b + cn \langle f_s(\mathbf{r}) \rangle_r)^2 \quad (6)$$

and its value at an intermediate time t_i after photophysical relaxation but before diffusion starts to influence the autocorrelation decay,

$$g_i \equiv g(t_i) = cn^2 \langle f_s^2(\mathbf{r}) \rangle_r + (b + cn \langle f_s(\mathbf{r}) \rangle_r)^2 \quad (7)$$

Knowing these three values, the number of emitters per molecule is calculated as

$$n = \frac{g_i - g_\infty}{g_i - g_0} \quad (8)$$

Still, when using pulsed excitation, the above considerations have to be modified. Now, we need the short time evolution of the function $f(\mathbf{r}, t)$ in eq 3 on a nanosecond time scale of the fluorescence lifetime. Assuming negligible laser pulse duration, the temporal evolution of $f(\mathbf{r}, t)$ can be written as

$$f(\mathbf{r}, t) = \frac{\kappa_0(\mathbf{r})}{\tau} \left[\exp\left[-\frac{\text{mod}(t, T_{\text{rep}})}{\tau}\right] - \exp\left(-\frac{t}{\tau}\right) \right] \quad (9)$$

where $\kappa_0(\mathbf{r})$ is a position-dependent factor accounting for excitation intensity, absorption cross section, fluorescence quantum yield, and detection efficiency; τ is the fluorescence lifetime; T_{rep} is the time between subsequent laser pulses. It is assumed that $\tau \ll T_{\text{rep}}$ and that t is much shorter than the photophysical relaxation time connected with intersystem crossing or other similar photophysical processes (e.g., cis-trans transitions). For pulsed excitation, the stationary function f_s is now also temporally modulated and reads

$$f_s(\mathbf{r}, t) = \frac{\kappa(\mathbf{r})}{\tau} \exp\left[-\frac{\text{mod}(t, T_{\text{rep}})}{\tau}\right] \quad (10)$$

where $\kappa(\mathbf{r})$ is a factor similar to $\kappa_0(\mathbf{r})$, however, taking into account the partial population of nonfluorescing molecular states after photophysical relaxation. Thus, on a nanosecond time scale, g_1 has the explicit form

$$g_1(t) = \langle \langle n f(\mathbf{r}, t_0 + t) f_s(\mathbf{r}, t_0) + n(n-1) f_s(\mathbf{r}, t_0 + t) f_s(\mathbf{r}, t_0) \rangle_{t_0} \rangle_r \quad (11)$$

where the inner angular brackets with subscript t_0 denote averaging over all time values t_0 . After explicitly carrying out this averaging, one obtains

$$g(t) = \frac{1}{2\tau} \left\{ \begin{aligned} & \langle n(n-1) \kappa^2(\mathbf{r}) + n \kappa_0(\mathbf{r}) \kappa(\mathbf{r}) \rangle_r \sum_{j=0}^{\infty} \exp\left[-\frac{|t - jT_{\text{rep}}|}{\tau}\right] - \\ & n \langle \kappa_0(\mathbf{r}) \kappa(\mathbf{r}) \rangle_r \exp\left(-\frac{t}{\tau}\right) \end{aligned} \right\} \quad (12)$$

In a similar way, one obtains for intermediate times the expression

$$g_i(t) = \frac{n^2}{2\tau} \langle \kappa^2(\mathbf{r}) \rangle_r \sum_{j=0}^{\infty} \exp\left[-\frac{|t - jT_{\text{rep}}|}{\tau}\right] \quad (13)$$

For the sake of completeness, we also give the ACF in the limit of large values of t , when g_1 has already decayed to zero:

$$g(t \rightarrow \infty) = b^2 + 2bcn \langle \kappa(\mathbf{r}) \rangle_r + \frac{c^2 n^2 \langle \kappa^2(\mathbf{r}) \rangle_r}{2\tau} \sum_{j=0}^{\infty} \exp\left[-\frac{|t - jT_{\text{rep}}|}{\tau}\right] \quad (14)$$

RESULTS AND DISCUSSION

A first set of measurements was performed on water solutions of the commercial dye Atto655. This dye has the remarkable property to show discernible intersystem crossing only at very high excitation intensities. This can be seen when inspecting Figure 1A, showing the ACF as measured on a ~ 1 nM solution of the dye. The autocorrelation does not show any short-term decay in the nano- and microsecond region that would indicate triplet-state population. Figure 1B shows a magnification of the ACF around zero lag time with 50-ps temporal resolution on a linear time scale. In all figures occurring in this paper, positive lag time values correspond to pair correlations of photons detected by the first detector against photons detected by the second detector, and negative lag time values correspond to pair correlations of photons detected by the second detector against photons detected by the first detector. Finally, Figure 1C shows a magnification, again with 50-ps temporal resolution, of the ACF at large lag times, $t + \Delta t$, where Δt was chosen to be 3 s, so that $g_1(t)$ has already completely decayed to zero (as also visible by looking at Figure 1A). Because Atto655 does not show any fast photophysical processes in its autocorrelation, the functions $\kappa_0(\mathbf{r})$ and $\kappa(\mathbf{r})$ occurring in eqs 12 and 13 are identical, making data analysis particularly simple. First, the correlation function at short times as presented in Figure 1B and at long times as presented in Figure 1C are simultaneously fitted by the model functions

$$A + B \sum_{j=0}^{\infty} \exp\left[-\frac{|t - jT_{\text{rep}}|}{\tau}\right] - C \exp\left(-\frac{t}{\tau}\right) \quad (15)$$

and

$$A' + B' \sum_{j=0}^{\infty} \exp\left[-\frac{|t - jT_{\text{rep}}|}{\tau}\right] \quad (16)$$

with fit parameters A , B , C , A' , B' , and τ . Because $\kappa_0(\mathbf{r})$ and $\kappa(\mathbf{r})$ are identical and thus also $\langle \kappa_0(\mathbf{r})\kappa(\mathbf{r}) \rangle$ and $\langle \kappa^2(\mathbf{r}) \rangle$, the number of independent emitters per diffusing molecule can be calculated as $n = (B - B')/C$ (cf. eqs 8, 12, and 13). We repeated the measurement on Atto655 solutions 10 times, each measurement lasting 15 min, and the resulting mean value plus/minus standard deviation of independent emitters per diffusing molecule is 1.01 ± 0.02 , thus in excellent agreement with the expected value of one.

The situation becomes more involved when the fluorophores exhibit significant photophysical relaxation. This is visible in Figure 2A, showing the ACF as measured for a ~ 1 nM aqueous

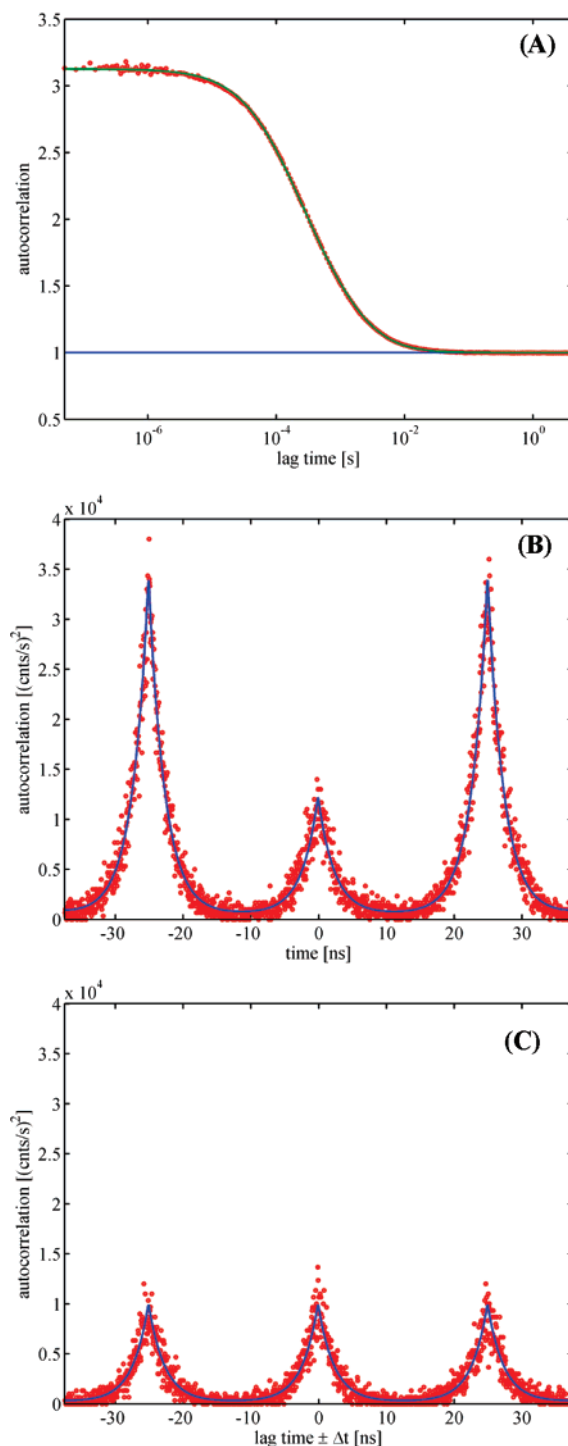


Figure 1. (A) Normalized measured ACF (circles) of a nanomolar solution of Atto655 in water. The temporal decay of the ACF is solely determined by the diffusion of the dye out of the detection volume; not fast photophysical relaxation is discernible on the microsecond time scale. The curve fit (solid line) was done using eq 17 but without the exponential terms. (B) Magnification of the ACF around zero lag time. Minimum temporal resolution is 50 ps. Positive lag time values correspond to pair correlations of photons detected by the first detector against photons detected by the second detector, and negative lag time values correspond to pair correlations of photons detected by the second detector against photons detected by the first detector. Curve fitting was done using eq 15. (C) Magnification of the ACF around a lag time of $\Delta t = 3$ s. Positive and negative lag time values have the same meaning as in (B). Minimum temporal resolution is again 50 ps. Curve fitting was done using eq 16. Total measurement time for the shown curves was 1.5 h.

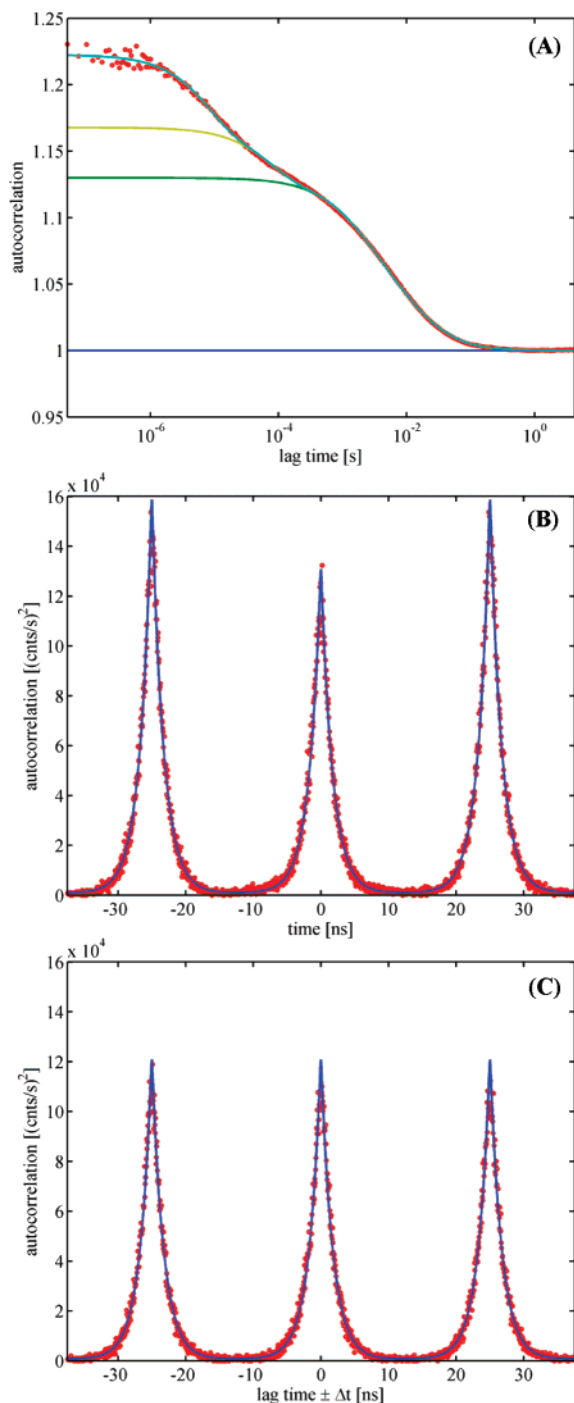


Figure 2. Same as Figure 1, but for a solution of Alexa647. Now, curve fitting in (A) was done by using the full eq 17. At least two exponential terms were needed to obtain a satisfactory fit quality. (A) shows also the fit components without the second and without both exponential terms (pure diffusional part of the ACF). Total measurement time for the shown curves was 1.5 h.

solution of the commercial dye Alexa647. The autocorrelation of Figure 2A was fitted with the standard model function

$$D + \left[E + F \exp\left(-\frac{t}{t_1}\right) + G \exp\left(-\frac{t}{t_2}\right) \right] \frac{1}{(1 + t_3/a) \sqrt{1 + t_4/b}} \quad (17)$$

with fit parameters D , E , F , G , t_1 , t_2 , t_3 , and t_4 . The parameters t_1 and t_2 describe the fast temporal decay of the ACF on a microsecond time scale, whereas the parameters t_3 and t_4 describe the long-time decay of the autocorrelation connected with the diffusion of the fluorescing molecules out of the detection volume. It should be mentioned that at least two exponentials were needed, as given in eq 17, for satisfactorily fitting the measured ACF. This is probably due to (i) the inhomogeneous excitation light distribution within the detection region, so that molecules at different positions within that volume exhibit different photophysical, excitation intensity-dependent relaxation dynamics, and (ii) by a complex intermingling of triplet-state dynamics and cis–trans conformation transitions of the dye Alexa647. However, for our purposes, the exact nature behind and details of the ACF are rather unimportant. What is needed from fitting the ACF is an estimate of the ratio between $\langle \kappa_0(\mathbf{r})\kappa(\mathbf{r}) \rangle$ and $\langle \kappa^2(\mathbf{r}) \rangle$. This ratio will be proportional to the short-time value of the ACF as shown in Figure 2A and its intermediate value after photophysical relaxation and before diffusion sets in. Thus, we estimate this ratio as

$$\frac{\langle \kappa_0(\mathbf{r})\kappa(\mathbf{r}) \rangle}{\langle \kappa^2(\mathbf{r}) \rangle} = \frac{D + F + G}{D} \quad (18)$$

Figure 2B and C again shows magnifications of the ACF around zero and around 3-s lag time, and these curves are fitted as before for Atto655. Now, taking into account eq 18, the number of independent emitters per diffusing molecule is calculated as

$$n = \frac{B - B'}{C} \frac{D}{D + F + G} \quad (19)$$

Again, we performed five measurements each lasting 18 min, and the resulting mean value plus/minus standard deviation of independent emitters per diffusing molecule is 1.09 ± 0.20 , in fairly good agreement with the correct value of one.

To check whether antibunching measurements in solution are indeed capable of determining the labeling stoichiometry of molecular complexes with more than one label, we prepared fluorescently labeled DNA double strands with known labeling stoichiometry. For this purpose, a 60-mer oligonucleotide and its two 30-mer counterstrands with covalently bound Oregon Green dye molecules at the 5'-ends were used. We measured the pure 60-mer (one label), the 60-mer with one hybridized 30-mer counterstrand (two labels), and the 60-mer with two hybridized 30-mer counterstrands (three labels). Excitation was now done at 470 nm, causing higher background, and fluorescence brightness of the molecules was now significantly lower than for the synthetic red dyes Atto655 and Alexa647. The fluorescence correlation and antibunching results for the three cases are shown in Figures 3–5. The determined number of fluorescent labels are 1.02 for the pure 60-mer, 1.8 for the 60-mer plus one 30-mer, and 2.9 for the 60-mer plus two 30-mers, in fairly good agreement with the expected values. When comparing the antibunching

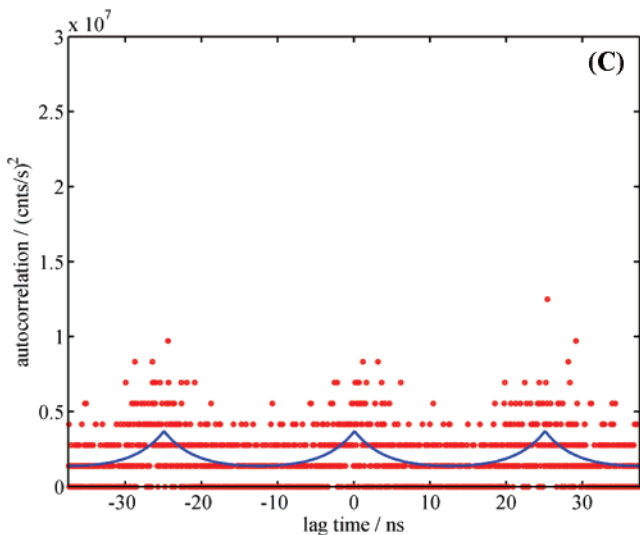
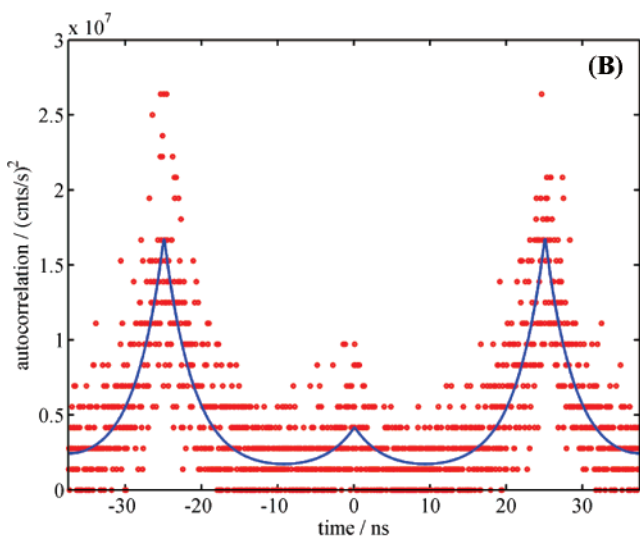
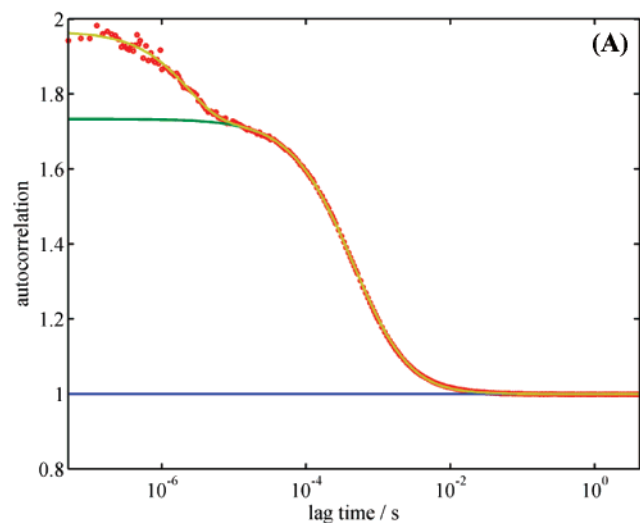


Figure 3. Same as Figure 2, but for an aqueous solution of a 60 oligomer labels with a single Oregon Green dye molecule. Total measurement time for the shown curves was 4 h.

curves of Figures 3–5B and C with Figures 1 and 2B and C, it is obvious that the fluorescence brightness of Oregon Green is significantly lower than that of Atto655 or Alexa647. Nonetheless,

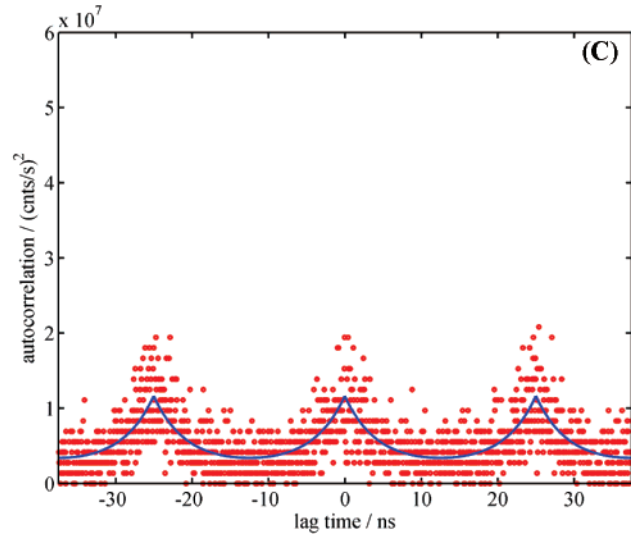
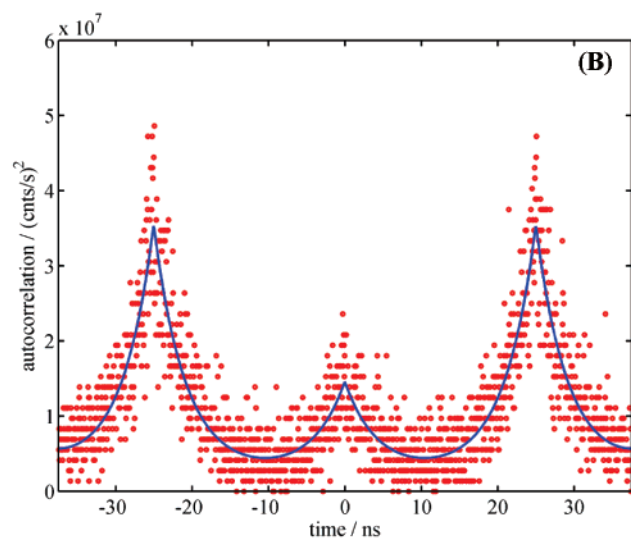
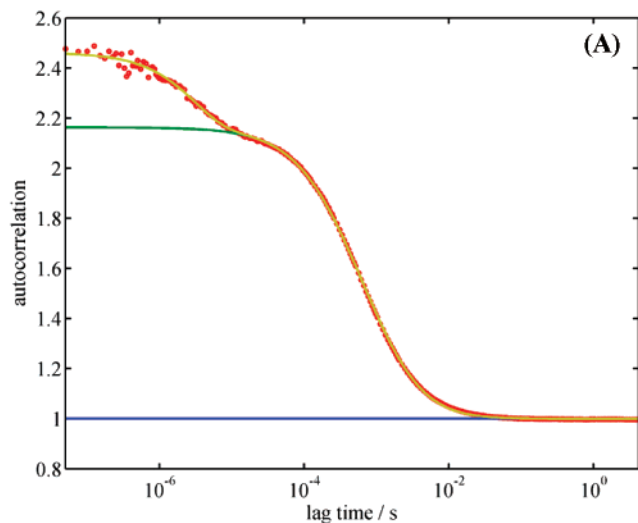


Figure 4. Same as Figure 2, but for an aqueous solution of a 60-oligomer hybridized with one 30-mer counterstrand, both labeled with a single Oregon Green dye molecule. Total measurement time for the shown curves was 4 h.

due to the integrating nature of the measurements, which accumulate signal over many individual molecule transits, antibunching measurements still lead to reasonable results, although

the measurement time of 4 h is now considerably longer than that for the dyes Atto655 and Alexa647.

Encouraged by these results, we extended our measurements to fluorescent proteins. We started with a pure aqueous solution of enhanced green fluorescent protein (EGFP). As for the Oregon Green-labeled oligomers, excitation was done at 470 nm. Figure 6 shows the measured correlation functions. In Figure 6B, a new technical problem can be seen, which occurs when detecting fluorescence in the emission band of EGFP: The prominent side peaks at $\sim \pm 8$ ns are caused by solid-state luminescence of the used silicon SPADs (detector afterglowing). Each time a SPAD is hit by a photon causing an electron avalanche, solid-state luminescence is generated that can be caught by the second detector (remember that all measurements are done by cross-correlating photons from the two detectors). Unfortunately, the spectrum of this luminescence overlaps with the EGFP emission, so that it is impossible to completely suppress its detection by using appropriate optical filters, as was possible when detecting in the red spectral region. To take these luminescence-caused side peaks into account, the empirical terms

$$H_+ t^{\alpha_L} \exp\left[-\frac{(t-t_L)}{\tau_L}\right] \quad \text{if } t > 0, \quad \text{and} \\ H_- |t|^{\alpha_L} \exp\left[-\frac{(|t|-t_L)}{\tau_L}\right] \quad \text{if } t < 0 \quad (20)$$

were added to the model function, eq 15, introducing the additional fit parameters t_L , τ_L , α_L , H_+ and H_- . Again, we repeated the measurement five times, but now each measurement lasting 1.2 h. The mean value plus/minus standard deviation of independent emitters per diffusing molecule was determined to be 1.07 ± 0.27 , again in fairly good agreement with the correct value of one.

As test samples for checking the method as a means of obtaining stoichiometric information on molecular complexes, we have chosen the ligand-gated ion channels (LGICs) P2X₁ and $\alpha 1$ glycine receptor (GlyR), which are known to form exceedingly stable homotrimers and homopentamers, respectively.^{31,32} C terminally EGFP-tagged versions of the His-rP2X₁ subunit or the GlyR $\alpha 1$ -His subunit were expressed in *Xenopus laevis* oocytes and purified from these cells by metal affinity chromatography in dodecyl maltoside-solubilized form, as described in the Materials and Methods section. Blue native PAGE analysis followed by visualization of the fluorescent proteins with a fluorescence scanner verified that His-P2X₁-EGFP receptors and GlyR $\alpha 1$ -His-EGFP receptors existed entirely as fully assembled homotrimers or homopentamers, respectively (results not shown). For each sample, we performed five measurements of 1.2-h duration. The obtained correlation functions are shown in Figures 7 and 8, together with their fits using eqs 15–17 and 20. The resulting mean value plus/minus standard deviation of independent emitters per diffusing molecule were determined to be 2.51 ± 0.09 for P2X₁, and 2.06 ± 0.06 for the GlyR receptor. Both values differ

(31) Nicke, A. H.; Bäumert, G.; Rettinger, J.; Eichele, A.; Lambrecht, G.; Mutschler, E.; Schmalzing, G. *EMBO J.* **1998**, *17*, 3016–3028.

(32) Griffon, N.; Büttner, C.; Nicke, A.; Kuhse, J.; Schmalzing, G.; Betz, H. *EMBO J.* **1999**, *18*, 4711–4721.

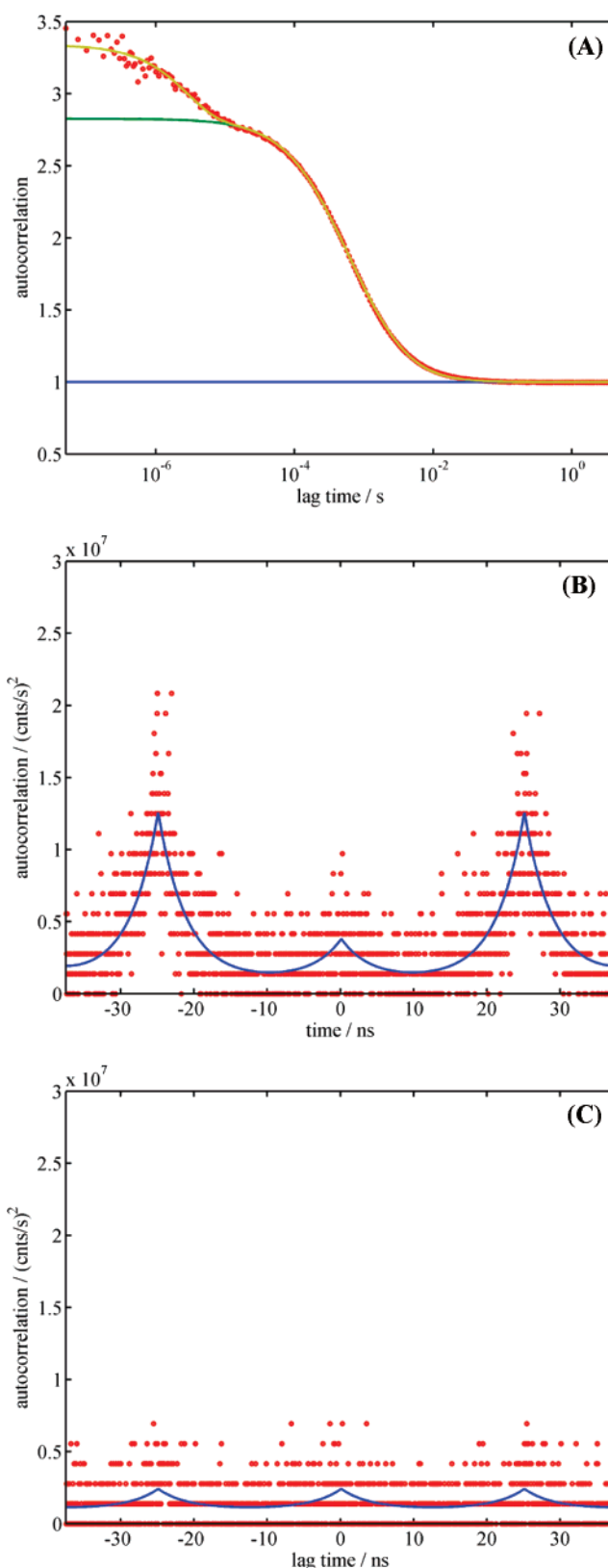


Figure 5. Same as Figure 2, but for an aqueous solution of a 60-oligomer hybridized with two 30-mer counterstrands, all labeled with a single Oregon Green dye molecule. Total measurement time for the shown curves was 4 h.

significantly from the expected values of 3 and 5, respectively. The relatively small standard deviation rules out a failure of the method's accuracy. There are several possible causes for the

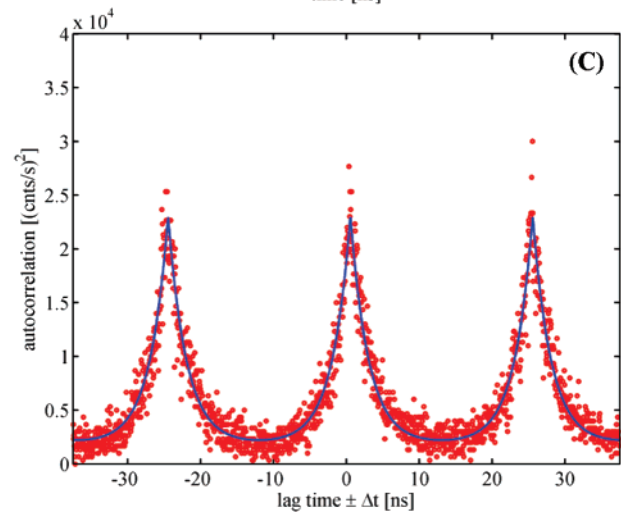
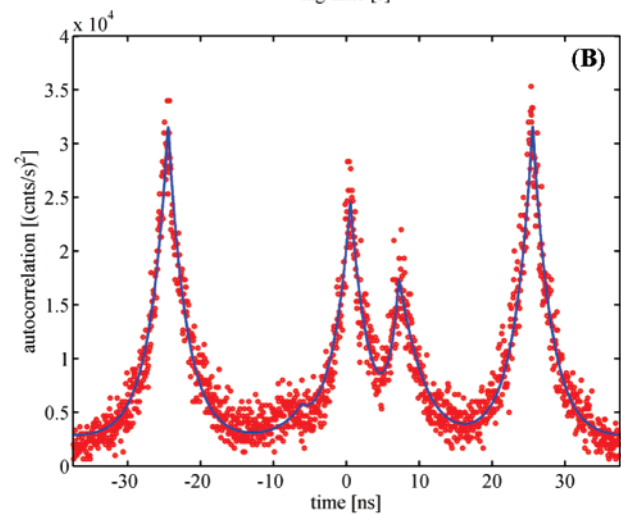
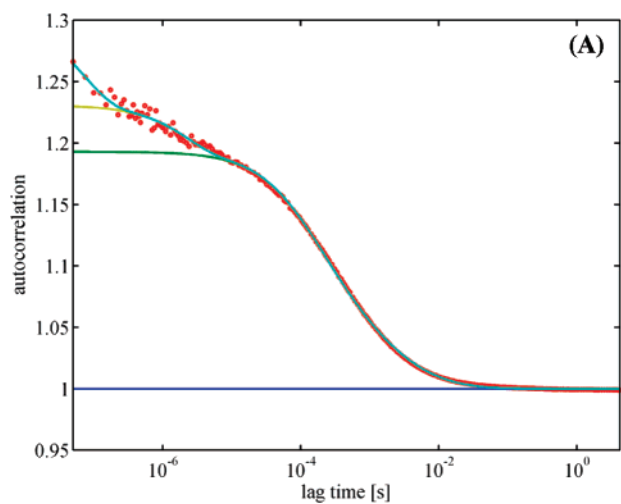


Figure 6. Same as Figure 2, but for a solution of EGFP. Now, curve fitting in (B) was done by using eq 15 plus the additional terms of eq 20. Again, two exponential terms were needed when fitting the ACF in (A) with the model eq 17. The fast exponential term is due to rotational diffusion. Total measurement time for the shown curves was 6 h.

disagreement between measured numbers of emitters per construct. The first is that not all fused EGFP molecules matured into a fluorescing conformation. A second case could be that the reconstituted constructs were not stable at nanomolar dilution,

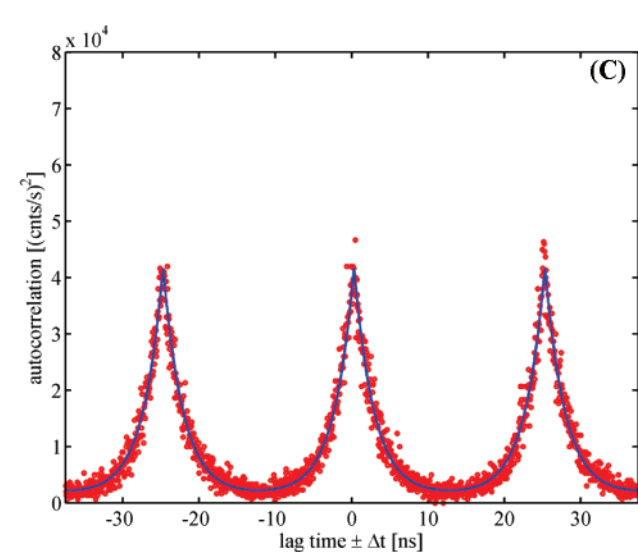
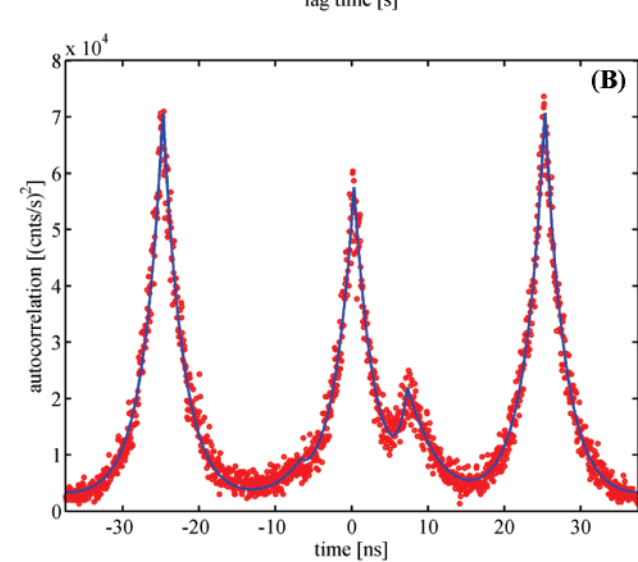
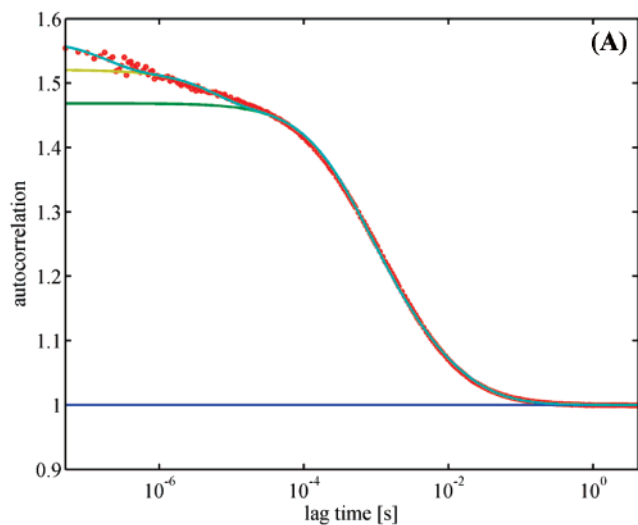


Figure 7. Same as Figure 6, but for a solution of dodecyl maltoside-solubilized homotrimeric P2X₁ receptor channels.

leading to a sample with an inhomogeneous distribution of labels per diffusing complex. In both cases, fluorescence antibunching will measure a weighted average of the labeling distribution. However, a third and the most probable source for the discrepancy

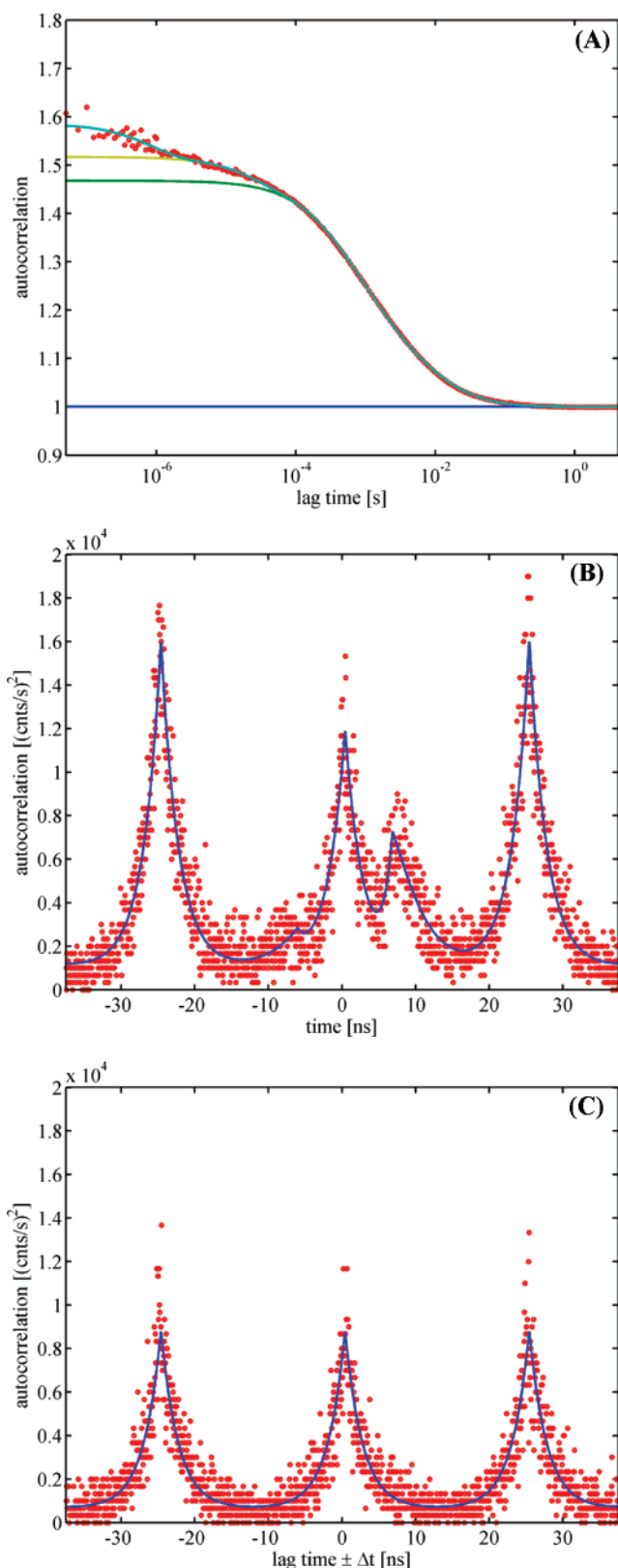


Figure 8. Same as Figure 6, but for a solution of dodecyl maltoside-solubilized homopentameric GlyR channels.

between determined and actual number of labels per complex could be photophysical coupling between different EGFP molecules. Using antibunching measurements on immobilized autofluorescent tetrachromophoric dsRed protein complexes, Sánchez-

Mosteiro et al.³³ found significant singlet–singlet annihilation of excitations between different chromophores, leading to the effect that the whole tetrachromophoric system behaves mostly like a single emitter although there are four absorption and potential emission sites per dsRed complex. Similar singlet–singlet annihilation was observed and extensively studied by antibunching in synthetic multichromophoric systems.^{26,27,29,30} Excitonic coupling between the EGFP labels leading to singlet–singlet annihilation would also bias the outcome of our antibunching-based determination of the number of EGFP molecules per diffusing complex.

CONCLUSIONS

In this paper, we have presented a method based on fluorescence antibunching providing information on the stoichiometry of molecular complexes, i.e., determines the average number of fluorescent labels per molecule or molecular complex diffusing in solution. The described method has the advantage that it accumulates antibunching data over many transits of diffusing molecules in solution, thus making antibunching measurements possible also for weakly fluorescing labels. Unlike other fluorescence approaches such as brightness analysis (PCH, FIDA), no calibration by a reference, e.g., a dye in the purely monomeric form, is needed. The validity of the method as well as of the data analysis was tested on free dye solutions of Atto655 and Alexa647, on multiply labeled double-strand oligomers, and on a solution of a green fluorescent protein (EGFP). The obtained values of emitters per molecule for all these systems correspond to the expected values. In addition, it is demonstrated that the obtained values are not altered by the photophysical behavior of various dyes.

Finally, we applied the method to two different, multiply EGFP-labeled biological molecular complexes, P2X₁ and GlyR, known to form homotrimers and homopentamers, respectively. The determined number of independent emitters per complex significantly differed from the expected values of three and five. The most probable cause of this discrepancy is excitonic coupling between the attached EGFP molecules. A solution to that problem could be to use longer linkers between the EGFPs and the labeled proteins, thus increasing the distance between different EGFP labels and decreasing their photophysical coupling, or to use fluorescent labels that do not show excitonic coupling. Two additional limitations of the method should be mentioned: first, antibunching measurements always require relative long measurements times and thus sufficiently stable samples. Second, it measures only an average number of labels per complex, so that antibunching in solution will be most useful for samples with rather homogeneous label stoichiometry. Nonetheless, we expect that fluorescence antibunching measurements in solution can be a powerful tool for measuring absolute numbers of subunits in biological complexes.

MATERIALS AND METHODS

Measurement System. The confocal microscope was described in detail in ref 34. A pulsed diode laser system (PDL 800, PicoQuant) generating pulses with 150-ps pulse width at 40-MHz

(33) Sánchez-Mosteiro, G.; Koopman, M. E.; van Dijk, M. H. P.; Hernando, J.; van Hulst, N. F.; García-Parajó, M. F. *ChemPhysChem* **2004**, *5*, 1782–1785.

(34) Böhmer, M.; Pampaloni, F.; Wahl, M.; Rahn, H. J.; Erdmann, R.; Enderlein, J. *Rev. Sci. Instrum.* **2001**, *72*, 4145–4152.

repetition rate was used for excitation. The light of the laser was sent through a single-mode waveguide and subsequently collimated to form a beam with Gaussian beam profile of 2.5-mm beam waist radius. The beam was spectrally filtered using a narrow-band excitation filter. The beam was then focused through an apochromatic oil immersion objective (60 \times , 1.45 NA, Olympus) into the sample solution. Fluorescence was collected by the same objective (epifluorescence setup) and then separated from the excitation light by a dichroic mirror. A tube lens with 180-mm focal length focused it onto a circular aperture of 100- μ m diameter. After the aperture, the light was split into two channels. After passing an additional bandpass filter, the light was refocused by achromatic lenses (60 mm, Linos) onto two single-photon avalanche diodes (SPCM AQR-13, Perkin-Elmer). A dedicated single-photon counting electronics (PicoHarp 300, PicoQuant) was used for recording and processing the detected photons from both detectors independently, allowing cross-correlation between photons from both detectors down to 8 ps.

For measurement of the fluorescent labels Atto655 and Alexa647, an excitation wavelength was 640 nm (LDH640). Excitation filter 640DF10 and dichroic 650DLRP (OmegaOptical) were used. Emission was detected through 690DF40 (Omega Optical) bandpass filters in front of each detector.

Measurement of Oregon Green-labeled oligomers was done using an excitation wavelength of 470 nm (LDH470). Excitation filter 475DF20 and a dichroic mirror 490DLRP (OmegaOptical) were used. Emission was detected through 510AF20 (Omega Optical) bandpass filters in front of each detector.

Measurement of EGFP and the protein complexes was done using an excitation wavelength of 470 nm (LDH470). Excitation filter 475DF20 and a dichroic mirror 505DLRP (OmegaOptical) were used. Emission was detected through 535AF26 (Omega Optical) bandpass filters in front of each detector.

Fluorescent Dyes and Labeling of the Oligonucleotides.

Oregon Green in the form of *N*-hydroxysuccinimidyl ester, 5-isomer (CAS Number 198139–51-4) was purchased from Invitrogen (Karlsruhe, Germany). A 60-mer oligonucleotide and its two 30-mer counterstrands with attached C6-amino modifier at the respective 5'-end were purchased from Operon Biotechnologies (Cologne, Germany). The respective sequences were (5' to 3') ATC GTT ACC AAA GCA TCG TAA ATC GCA TAA TAG CAC GTT AAT TTA GCA CGG ACG ATC GCC, TTA TGC GAT TTA CGA TGC TTT GGT AAC GAT and GGC GAT CGT CCG TGC TAA ATT AAC GTG CTA.

Labeling of the C6-amino linkers of the oligonucleotides with the fluorescent dyes was performed following the recommended protocol. To 1 mol equiv of oligonucleotide, a 5-fold excess of activated dye was added, dissolved in 0.1 M borate buffer (pH 8.5) and stirred for 6 h in the dark. Nucleotides were precipitated

and washed twice with cold ethanol. The remainder was dissolved in TE buffer (10 mM Tris, 1 mM EDTA, pH 8.0) and further purified by HPLC using a BioSep-SEC-S 200 size exclusion column from Phenomenex (Aschaffenburg, Germany). Hybridization of the labeled oligonucleotides was accomplished by heating equimolar amounts in TE buffer to 85 °C and cooling to room temperature (25 °C) over 3 h. After hybridization, the products were purified again by gel filtration. For measuring, the samples were diluted in TE buffer to nanomolar concentrations.

cDNA Constructs. The complete open reading frame (ORF) of EGFP was PCR-amplified from the pEGFP-C1 vector (Invitrogen) and directionally subcloned into the oocyte expression vector pNKS2.³⁵ Codons for a hexahistidyl (His) sequence were inserted by QuikChange site-directed mutagenesis (Stratagene, La Jolla, CA) immediately downstream of the initiator ATG to yield His-EGFP-pNKS2 encoding the EGFP fluorescent protein with an N-terminal His tag. Constructs encoding EGFP fusion proteins of LGICs were generated by using two constructs from previous work, His-rP2X₁-pNKS2³¹ and GlyR α 1-His-pNKS2,³² which encode the rat P2X₁ subunit and the GlyR α 1 subunit with N-terminal or C-terminal His-tags, respectively. The EGFP coding region was directionally inserted at the 3' end of the ORFs of both genes, thus yielding His-rP2X₁-EGFP and GlyR α 1-His-EGFP. Insertions and junctions of these constructs were verified by restriction fragment analysis and fluorescence sequencing.

Oocyte Expression and Native Purification of EGFP and EGFP-Tagged LGICs. Capped cRNAs were synthesized from linearized plasmid templates and injected into defolliculated *X. laevis* oocytes, which were kept at 19 °C. After 1–2 days, His-tagged proteins were purified by Ni²⁺ nitrilotriacetic acid (NTA) agarose (Qiagen, Hilden, Germany) chromatography from dodecyl maltoside (0.2%) extracts of these oocytes as detailed previously.^{31,32} Two additional washing steps with 0.05% dodecyl maltoside in phosphate-buffered saline served to remove any residual imidazole contained in the initial washing buffer from the Ni²⁺ NTA beads before protein elution. Proteins were eluted from Ni²⁺ NTA agarose with a nondenaturing solution consisting of 100 mM EDTA (pH 7.4 with NaOH) and 0.05% dodecyl maltoside, and then kept at 0 °C until analysis.

ACKNOWLEDGMENT

This work was supported by grants of the Deutsche Forschungsgemeinschaft to G.S. (Schm 536/6 and Schm536/7). J.S. greatly acknowledges support by the Ministry of Education of the Czech republic via grant LC06063. J.S. also thanks the Forschungszentrum Jülich for financing his stay as guest scientist at this institution.

Received for review October 30, 2006. Accepted April 2, 2007.

AC062024F

(35) Gloor, S.; Pongs, O.; Schmalzing, G. *Gene* **1995**, *160*, 213–217.